Thin Solid Films 589 (2015) 315–321

Contents lists available at ScienceDirect

Thin Solid Films

journal homepage: www.elsevier.com/locate/tsf

Ion-induced pattern formation on indium tin oxide for alignment of liquid crystals

T. Škereň [a,b,*], D. Doornaert [c,d], C. Glorieux [c], H. Modarresi [a], T. Guan [e], K. Temst [a], W. Vandervorst [a,f], A. Vantomme [a]

[a] Instituut voor Kern-en Stralingsfysica, KU Leuven, Celestijnenlaan 200D, B-3001 Leuven Belgium
[b] Czech Technical University in Prague, Faculty of Nuclear Sciences and Physical Engineering, Břehová 7, 115 19 Prague 1, Czech Republic
[c] Laboratory for Acoustics and Thermal Physics, Department of Physics and Astronomy, KU Leuven, B-3001 Heverlee, Belgium
[d] Wave Propagation and Signal Processing Research Group, KU Leuven Campus Kortrijk, E. Sabbelaan 53, B-8500 Kortrijk, Belgium
[e] Departement Elektrotechniek ESAT-MICAS, KU Leuven, Kasteelpark Arenberg 10, B-3001 Leuven, Belgium
[f] IMEC, Kapeldreef 75, B-3001 Leuven, Belgium

ARTICLE INFO

Article history:
Received 8 August 2014
Received in revised form 16 April 2015
Accepted 22 May 2015
Available online 29 May 2015

Keywords:
Ripple formation
Ion-induced pattern formation
Liquid crystal alignment
Indium-tin oxide

ABSTRACT

Indium tin oxide (ITO) is broadly used as a transparent conducting material for electrodes in optoelectronic devices. Irradiation of ITO with low energy ions can result in the formation of periodic surface nanopatterns which can serve as an alternative for the polymer alignment layer in liquid crystal devices. We investigated the formation of the ion-induced surface nanopatterns on ITO with focus on the influence of the crystalline structure of the material. We find that the crystallinity plays a crucial role in the pattern formation, with no pattern developing on an amorphous ITO surface. We discuss these findings in the context of the state-of-the-art theory for ion-induced patterning. We show that the ion-induced pattern plays a critical role in the liquid crystal alignment on ITO surfaces.

1. Introduction

Irradiation of surfaces with low energy ions often leads to the formation of periodic surface nanostructures [1–4]. This phenomenon has recently attracted a lot of attention as a potentially powerful tool to fabricate surface nanostructures on large scale areas for various purposes [5–9]. Among the wide variety of applications, several studies demonstrated the possibility to use the ion-induced nanostructures for the alignment of liquid crystals [7,8,10–13].

Currently, liquid crystal (LC) optoelectronic device fabrication represents a massive and still growing industry. Substantial effort in this area is dedicated to the development of technology to improve the performance of the devices and simplify and reduce the costs of the fabrication process. LC devices rely on the optical anisotropy of a nematic liquid crystal layer, whose director needs to be strongly and uniformly aligned. In the absence of an electric field, planar alignment is typically achieved by orienting forces at the interfaces between which the LC is sandwiched. Switching on an electric field then induces a competitive orienting force, leading to a homeotropic or twisted nematic director pattern. A crucial task in the LC device fabrication is the treatment of the interfaces.

The most common industrial way of achieving this is by 1) depositing a polyimide (PI) thin film on the desired surface and 2) mechanically rubbing it in a specific direction. The rubbing process induces grooves along the polymer surface, resulting in an anisotropic surface texture, and alignment of LC molecules nearby the surface with the director along the rubbing and groove direction. One of the alternatives for this process is ion-induced patterning [8,10–12,14,15]. This technique is capable of producing an anisotropic nanoscopic surface morphology and surface anchoring of the LC molecules, and thus induce anisotropic alignment.

Ion-irradiation induced LC alignment has been applied on polyimide coated surfaces [8,10]. The PI film is usually deposited directly on the (transparent) electrodes of the LC devices, which are typically made of indium-tin-oxide (ITO). However, in the fabrication process, the deposition of PI represents an additional processing step, which could be avoided if the LC alignment was achieved directly by the ITO surface. Ion-induced nanopatterning of ITO thus has a high application potential in the LC device industry.

In this paper we study in detail the pattern formation on different ITO surfaces subjected to grazing incidence ion irradiation. At these conditions, formation of ripples parallel to the ion beam direction (so-called perpendicular mode ripples (PeMR) due to the orientation of the ripple

* Corresponding author at: V Holešovičkách 2, Praha 7, Czech Republic. Tel.: +420 221 912 817; fax: +420 284 684 818.
E-mail address: tomas.skeren@fjfi.cvut.cz (T. Škereň).

http://dx.doi.org/10.1016/j.tsf.2015.05.048
0040-6090/

wavevector) has been observed [5–7]. Formation of PeMR structure is typically associated with metallic surfaces while for amorphizable surfaces this ripple mode is either not present at all or the ripple pattern has very low quality. Specifically, we compare the PeMR pattern formation on amorphous and polycrystalline ITO and we conclude that the crystalline structure strongly influences the ripple pattern formation. These results are discussed in the context of the existing theory for the ion-induced patterning and possible causes for the dramatic difference between the patterning of amorphous and polycrystalline ITO are identified. It is also shown that the ion-induced morphology plays a critical role in the liquid crystal alignment.

2. Experimental details

We investigated the pattern formation on two different ITO samples. The polycrystalline Sample A was a sputter-deposited ITO film with a thickness of 240 nm purchased from Sigma-Aldrich. The amorphous Sample B was prepared by sputter-deposition at room temperature without any post-growth thermal treatment. The thickness of sample B, measured by Rutherford backscattering spectrometry, was 400 nm. This value may be somewhat underestimated since the possible porosity of the samples was not taken into account. The precise film thickness is, however, not critical for the current study.

Ion irradiation was performed with a 5 keV Ar^+ ion beam coming from an electron ionization ion gun. A weakly focused (~0.5 mm) ion beam with the current of 2.5 μA was scanned over an area of 9×9 mm^2. In order to achieve identical irradiation conditions, the two samples were placed next to each other on the same sample holder and irradiated simultaneously. Characterization of the sample surface was performed in situ by a scanning tunneling microscope (STM) prior to the irradiation and then after each irradiation step.

In order to investigate the liquid crystal alignment, two (identical) surfaces were put together facing each other and separated by a sheet spacer with a thickness of 20 μm. In the case of ion-irradiated surfaces the cells were assembled such that the irradiation directions of the two surfaces were anti-parallel. A droplet of E7 LC mixture was placed at the edge of the cell cavity, leading to capillary filling of the the cavity with the LC. The LC alignment in the cavity was then investigated by polarized light microscopy. E7 is a uniaxial positive liquid crystal with ordinary and extraordinary refractive index of 1.52 and 1.74 respectively.

3. Results

3.1. ITO film characterization

Figs. 1 and 2 respectively show the initial surface morphology of the two films and the $\theta - 2\theta$ X-ray diffraction (XRD) pattern of the two

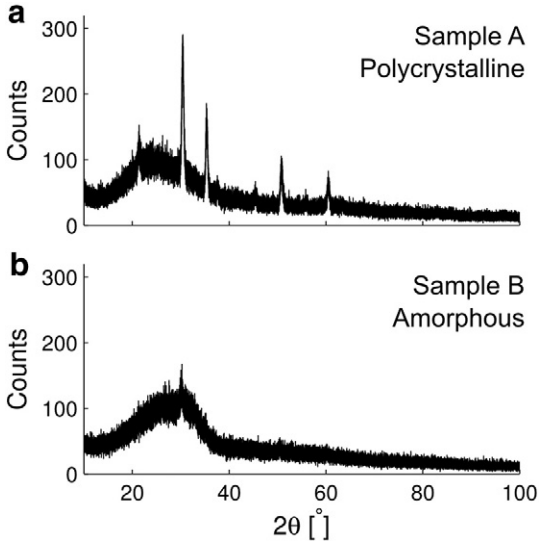

Fig. 2. θ–2θ XRD scans of a) sample A and b) sample B.

films (measured with Cu K-α X-ray source). The broad peak in the XRD pattern (between ~15°–40°) corresponds to the amorphous glass substrate. The strongest ITO diffraction peak is expected at 30.5° [16]. The XRD pattern of sample A reveals pronounced crystalline peaks while in the pattern of sample B only the strongest ITO peak is detectable, but with a substantially lower intensity. Since the layer thickness of the amorphous sample B was almost twice as large as the one of sample A, this implies that the amount of crystalline ITO in sample B was substantially smaller than in sample A. These observations are in agreement with previous studies on the crystalline structure of ITO surfaces sputter-deposited at different temperatures. [17–23].

The initial root mean square (RMS) roughness measured by STM is 2.2 nm for sample A and 3.4 nm for sample B.

3.2. Ion-induced pattern formation

Samples A and B were simultaneously irradiated by a grazing incidence 5 keV Ar^+ ion beam with gradually increasing ion fluence. The ion beam angle of incidence was 80°, measured from the surface normal (i.e. grazing incidence). STM topographs of the two surfaces after ion irradiation are presented in Fig. 3. A pronounced ripple pattern was formed on the surface of sample A with a direction parallel to the ion beam projection to the sample surface. This topography is visible even at the lowest ion fluence – 121 ions · nm^{-2} – and remains visible and comparable until the highest fluence studied here — 484 ions · nm^{-2}.

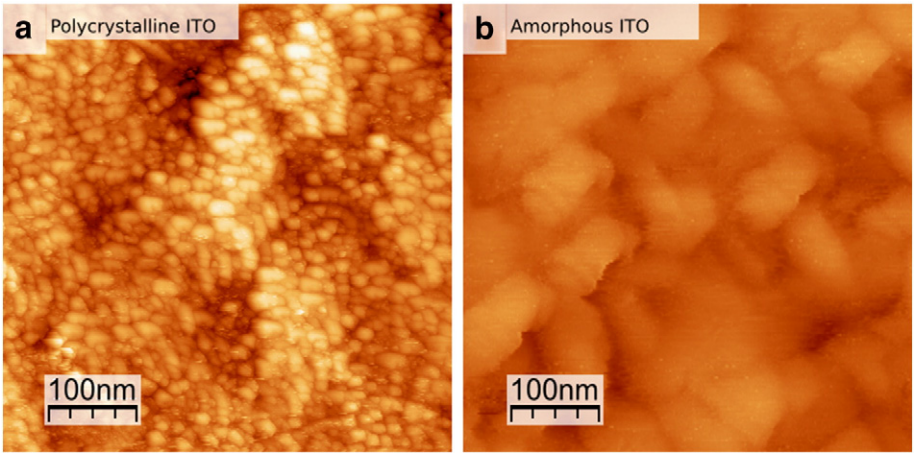

Fig. 1. Initial surface morphology of a) polycrystalline (sample A) and b) amorphous (sample B) ITO.

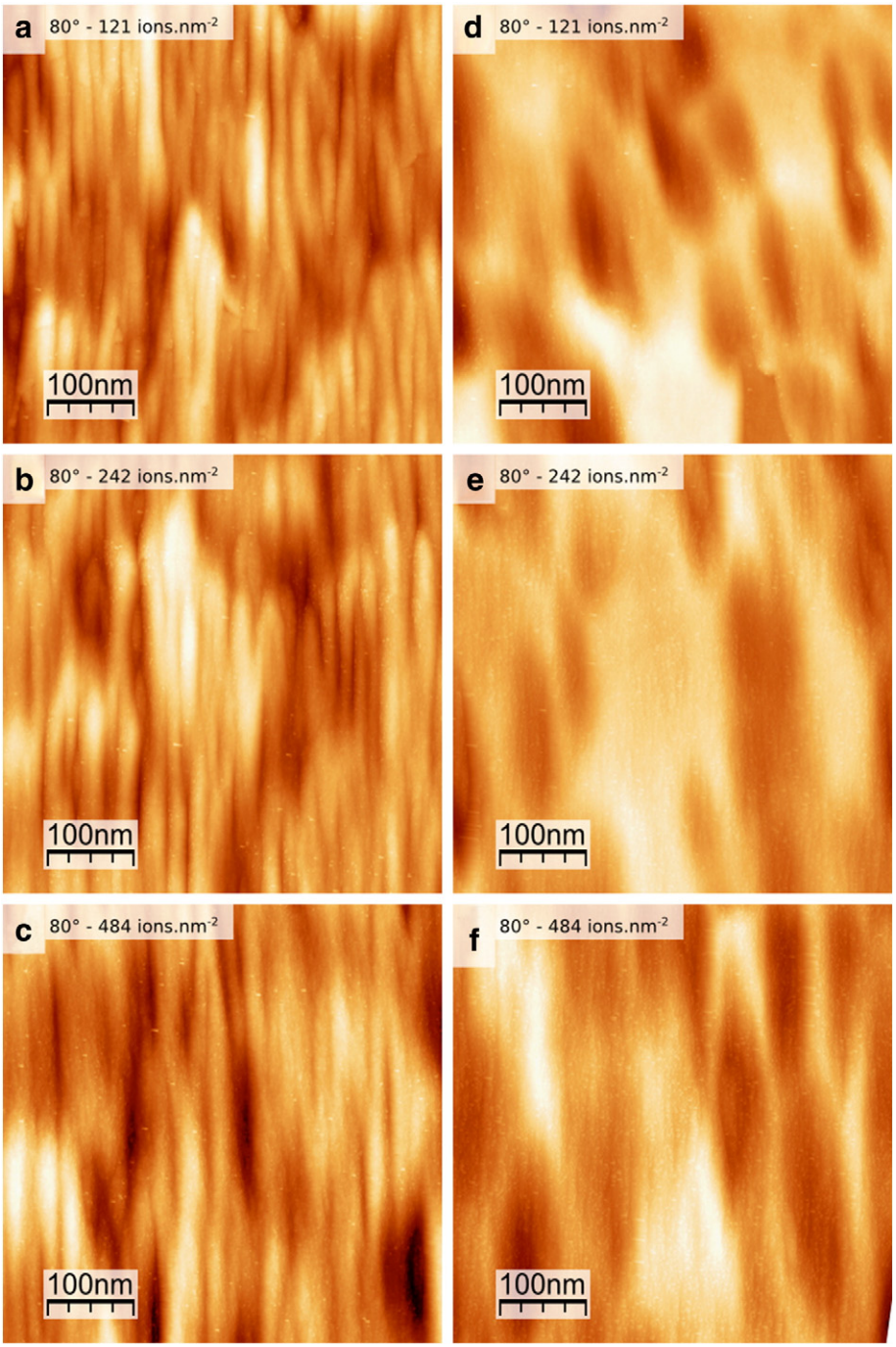

Fig. 3. 500 × 500 nm^2 STM topographs of the evolution of the surface morphology by grazing incidence ion irradiation of a–c) polycrystalline ITO surface and d–f) amorphous ITO surface.

On the other hand, the surface of sample B develops only a vague slightly anisotropic topography with shallow depressions elongated in the direction parallel to the ion beam. This elongation seems to become more pronounced with increasing ion fluence but no obvious ripple topography can be observed.

3.3. Optical measurements

To study the degree of liquid crystal alignment induced by the ITO surfaces we constructed different LC cells and investigated them by polarized light microscopy. The cells were rotated between crossed polarizers (analyzer and polarizer directions were perpendicular) and changes in optical transmission (cell brightness) were investigated. If the LC within the cell is disordered, then no net change of optical transmission is expected. If the LC has uniform planar alignment, then it exhibits (uniform) birefringence with the optical axis lying within the plane of the cell. The cell appears darkest if the entering light polarization is parallel or perpendicular to the optical axis and it appears brightest if the polarization is 45° from the optical axis.

In the case of untreated ITO surface no LC alignment was observed (Fig. 4a,d shows the polycrystalline ITO cell). Ion-irradiated polycrystalline ITO surface induced uniform planar alignment to the LC (Fig. 4b,e) shows a uniform change of the cell transmission by changing irradiated amorphous ITO surface does not induce uniform alignment and only small domains of aligned LC are present in the cell (Fig. 4c,f).

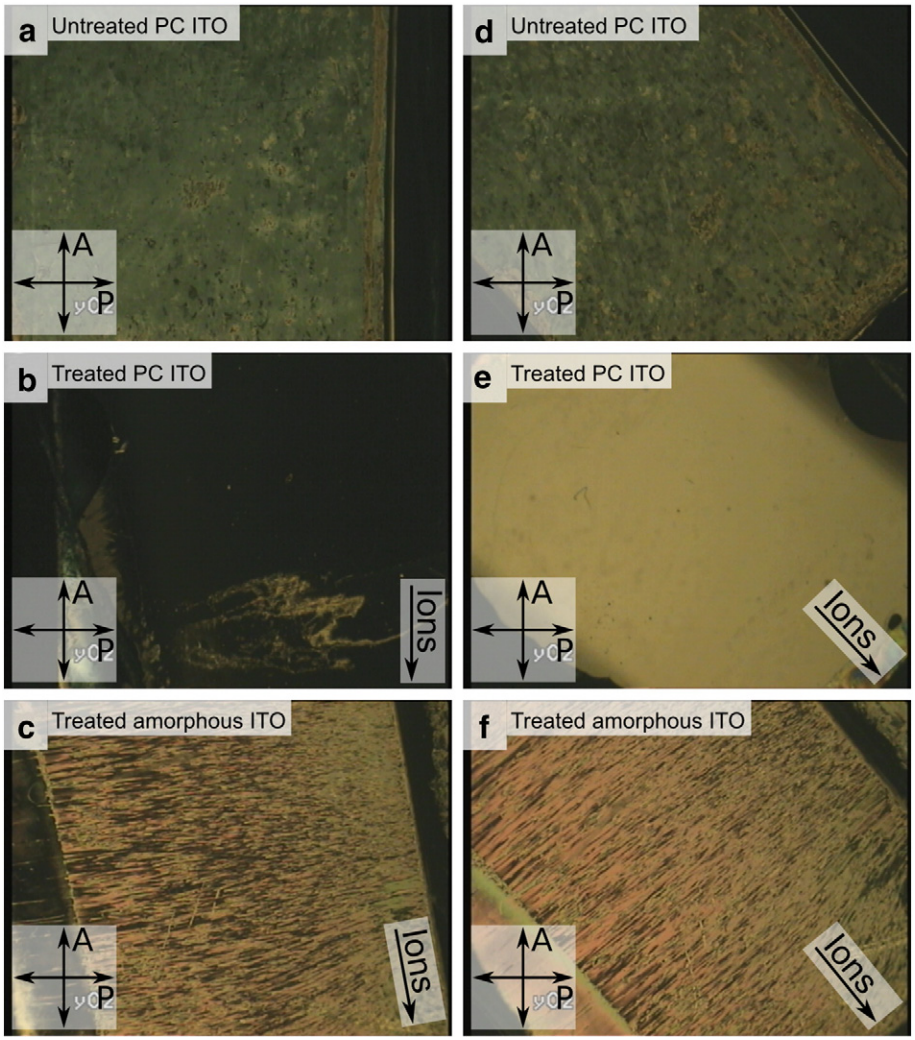

Fig. 4. Optical polarization microscopy images of LC cells constructed with a, d) untreated polycrystalline ITO surfaces, b, e) polycrystalline ITO surface irradiated with 5 keV Ar^+ ions to a fluence of 484 ions · nm^{-2} at 80° angle of incidence (direction indicated) and c, f) amorphous ITO surface irradiated at identical conditions as the latter.

4. Discussion

In the following we first discuss the possible causes of the different behaviors of the two surfaces and the likely mechanism of the ripple morphology formation for the polycrystalline ITO film. Next, we discuss the influence of the ion-induced surface morphology on the liquid crystal alignment.

4.1. Ripple pattern formation mechanism

4.1.1. Ion-induced linear instability

The difference in the patterning behaviors between the two samples is striking. Ripple pattern formation is conventionally described by the Bradley–Harper (BH) theory [24]. This theory attributes the pattern formation to an interplay between smoothening action of surface diffusion and a roughening effect, which results from the dependence of the sputter yield on the local surface curvature. This theory does not take into account the crystalline structure of the material and the only material property that determines the pattern formation is the character of the collision cascade. Since the two samples studied here have basically an identical chemical composition, this theory can hardly account for the dramatic difference in the pattern formation. In other words, if we assume that the ripple pattern on sample A is caused by the BH erosive instability, then there is hardly any reason why a similar pattern does not develop on the amorphous surface of sample B.

The importance of the erosive BH linear instability has been recently challenged: it was claimed [25,26] that in certain systems the erosive BH instability is essentially unimportant and the pattern formation is rather caused by material redistribution. However, the material redistribution does not easily explain the difference between the two samples either.

If the ripple topography of sample A is not caused by linear instability (either erosive or redistributive), then the question remains what mechanism stands behind the ripple formation and why this mechanism is not active for sample B.

4.1.2. Initial surface morphology

One obvious difference between the two samples (besides the crystalline structure) is the initial morphology of the surface. Their roughness is moderately different in magnitude, with a substantial difference in length scale (Fig. 1). The initial surface morphology has been shown to play an important role in the pattern formation [27–30]. It has been observed previously that the initial surface length scale is to a certain extent inherited by the ripple pattern that later develops on the surface [30]. Indeed, Figs. 1 and 3 show that the ripple pattern periodicity corresponds to the length scale of the initial surface.

However, the hypothesis that the initial surface morphology is the only reason for the difference between A and B is not entirely satisfactory. Previous studies indicate that the initial morphology decays after some erosion time, and the ripple pattern is expected to gradually fade away [31]. In case A the ripple pattern, however, seems to be stable

and neither wavelength, correlation length nor roughness of the pattern change substantially with the increasing ion fluence. The RMS roughness decreases from an initial 2.2 nm to 2 nm after the first irradiation step (121 ions/nm^{-2}) but then remains constant in the investigated fluence range. It is possible that the decay of the initial roughness is very slow and not observable in the fluence range of our experiments. However, the maximum fluence of 484 ions/nm^{-2} corresponds to the erosion of few tens of nanometers of material and it seems unlikely that the roughness would remain constant if no additional roughening mechanism was involved. This additional mechanism should cause roughening of sample A but it should be inactive for sample B.

4.1.3. Sputter yield variation in polycrystalline films

Multiple studies have reported the formation of a ripple pattern by grazing incidence ion irradiation of polycrystalline metallic surfaces [6,27,30,32–34,34]. We have previously studied the pattern formation on a polycrystalline Ni surface and proposed a mechanism to explain the pattern formation on this surface [35]. This mechanism is based on two components: 1) roughening of the eroded surface due to minor variation in the sputter yield between differently oriented grains and 2) non-linear erosion terms resulting from variation in the local ion flux and sputter yield due to varying slope on a roughened surface. The roughening is active at all angles of incidence but at grazing incidence the non-linear terms become sufficiently strong and they induce an anisotropy to the morphology evolution, which eventually leads to the formation of a ripple pattern. The patterning behavior on polycrystalline surfaces was shown to be in quantitative agreement with the predictions of this model [35].

The observations on amorphous and polycrystalline ITO correspond well to the expectations based on this model:

- The polycrystalline sample exhibits the formation of ripple structure because the random crystalline orientation induces minor variations to the sputter yield of different grains. This variation leads to the formation of roughness on the surface. By grazing incidence, the non-linear terms introduce an elongating tendency and convert the isotropic roughness into ripples parallel to the ion beam. The size of the crystal grains can be estimated from the XRD pattern using the Scherrer formula. The width of the XRD peak at 30.5° after correction for the instrumental broadening is 0.35° which gives an approximate size of the crystallites of about 30 nm. The wavelength of the ripples on sample A can be measured by the Fourier transform of the image and gives also a value of 30 nm. The precise agreement is clearly coincidental, given the approximative nature of Scherrer formula and unclear link between the grain size and precise ripple wavelength, however, this estimation confirms that the grain structure has indeed the same length scale as the observed ripples.
- The amorphous sample B exhibits some roughness on a larger scale but the ripple pattern observed on crystalline sample A is not present. Since the amorphous ITO is (ideally) homogeneous and there is no variation of the sputter yield, the mechanism described above is not active and the amorphous sample surface should remain flat. This is consistent with the observed evolution of the RMS roughness for sample B — from the initial value of 3.4 nm the RMS roughness gradually drops down to 1.9 nm throughout the sputtering process. The shallow anisotropic morphology, which is eventually observed on the surface, is either a relict of the initial surface morphology (being "stretched" by the same non-linear terms as describe above) or it can be ascribed to some fluctuation in the sample structure or composition that induces minor inhomogeneity to the erosion process and acts as a source of roughness but on a substantially larger scale than in sample A.

The sputter yield variation between differently oriented grains of the polycrystalline metals was attributed to the channeling phenomenon. Some grains are irradiated along a low-index direction, which lowers the sputter yield and these grains then protrude from the surface and induce roughening [35]. This mechanism requires that the material remains crystalline upon the ion irradiation (i.e. does not amorphize). This condition is fulfilled for the metallic surfaces but in the present case of ITO surface no experimental data showing the degree of crystalline damage for the current irradiation conditions are available.

In order to visualize any inhomogeneity in the sputter yield between different areas of the samples, we irradiated the two samples (previously patterned, corresponding to Fig. 3c,f) with an ion beam at low angle of incidence — 45°. In Fig. 5a,c) the surfaces of the two samples are presented. Both topographies show the formation of certain elevated or depressed "patches" on the surface. These patches point to the inhomogeneous structure of the material (in both cases), which causes the inhomogeneous erosion and the formation of roughness. Sample B (Fig. 5c) shows more or less homogeneous coverage of these patches with a nanoscopic roughness which is more clearly visible after edge-detection image processing (Fig. 5d). However, sample A reveals a coarser rough structure within the larger patches (Fig. 5b) which likely corresponds to the grain structure of the polycrystalline ITO film.

Regardless of the reason for the variation of the sputter yield, the protruding grains are expected to cause the formation of ripples at grazing incidence [35] and the polycrystalline sample is thus expected to exhibit similar behavior as that observed on the polycrystalline metal surface.

4.2. Liquid crystal alignment

As presented in Fig. 4 the interaction of the liquid crystal with the ion-irradiated ITO surface is very different between the two ITO surfaces. In the case of the amorphous ITO film, where the quality of the ion-induced ripple pattern was poor, no alignment of LC is observed. On the other hand, the pronounced ripple pattern on the polycrystalline surface induces uniform planar alignment. The ion-induced ripple pattern thus plays a critical role in the liquid crystal alignment.

5. Conclusions

We investigated the ion-induced pattern formation on amorphous and polycrystalline ITO surfaces and found that the crystalline structure plays a critical role in the development of the ripple morphology. A pronounced ripple pattern develops on the polycrystalline surface whereas the amorphous surface does not develop this ripple morphology. We showed that the ripple morphology is required to induce the alignment in liquid crystal.

The different patterning behavior of the amorphous and polycrystalline ITO is consistent with the mechanism of pattern formation, which was previously proposed for the patterning of polycrystalline metals — the polycrystalline material is eroded unevenly which induces the formation of surface roughness. The roughness is subsequently translated into a ripple pattern by non-linear effects resulting from the oblique ion irradiation. In contrast, the amorphous surface is eroded homogeneously and the ripple pattern does not develop. However, the detailed mechanism of the sputter yield variation in the polycrystalline ITO film may be different from the case of polycrystalline metals and has to be further investigated.

These results also have important practical consequences: careful attention has to be paid to the crystalline structure of the ITO if the formation of the ion-induced pattern is desired. This introduces an important condition for the ITO surfaces when applying the ion-induced structures for liquid crystal alignment.

Acknowledgments

This work was funded by the FWO, Vlaanderen, the KU Leuven (GOA/09/006 and GOA/14/007) and the European Commission through the SPIRIT (Support of Public and Industrial Research using Ion beam

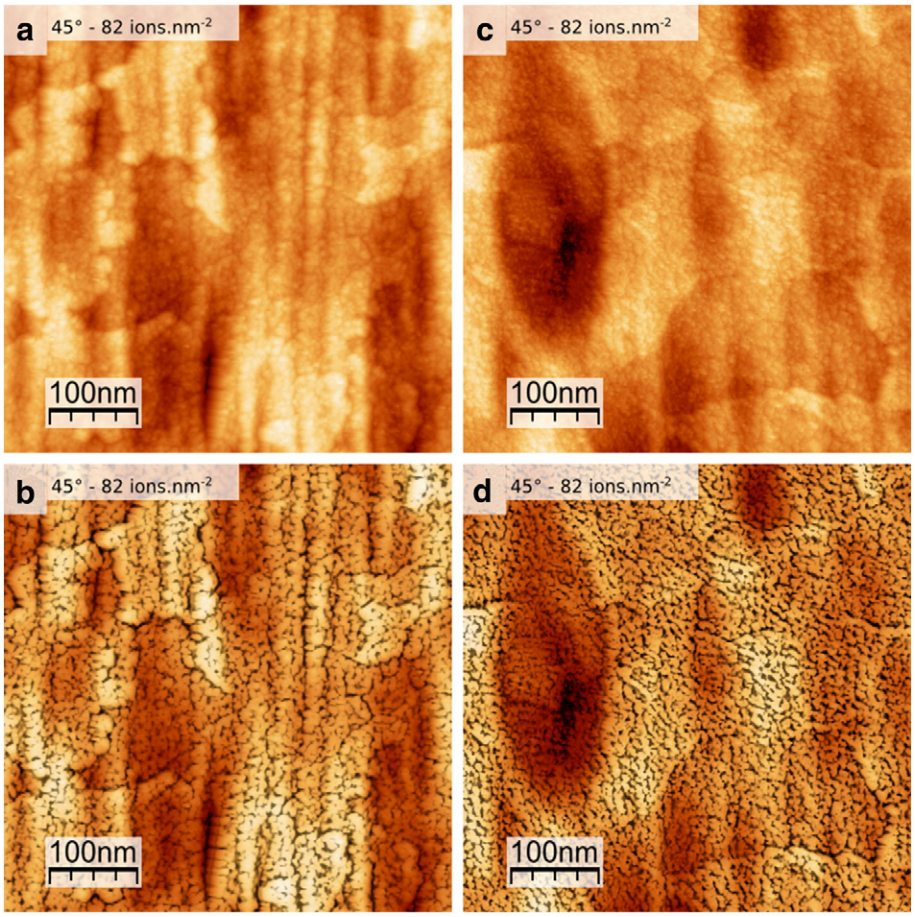

Fig. 5. STM topographs of a) polycrystalline and c) amorphous ITO surfaces after grazing incidence irradiation followed by 45° angle of incidence irradiation. b, d) show the same surfaces with enhanced edge-detection contrast.

Technology, Contract 227012) projects. Christ Glorieux acknowledges KU Leuven for financial support (research project OT/11/064).

References

[1] A. Keller, S. Facsko, W. Möller, Evolution of ion-induced ripple patterns on SiO_2 surfaces, Nucl. Instrum. Meth B267 (2009) 656–659.
[2] W.L. Chan, E. Chason, Making waves: kinetic processes controlling surface evolution during low energy ion sputtering, J. Appl. Phys. 101 (2007) 121301.
[3] S. Facsko, T. Dekorsy, C. Koerdt, C. Trappe, H. Kurz, A. Vogt, H.L. Hartnagel, Formation of ordered nanoscale semiconductor dots by ion sputtering, Science 285 (1999) 1551–1553.
[4] U. Valbusa, C. Boragno, F.B. de Mongeot, Nanostructuring surfaces by ion sputtering, J. Phys. Condens. Matter 14 (2002) 8153–8175.
[5] F. Buatier de Mongeot, U. Valbusa, Applications of metal surfaces nanostructured by ion beam sputtering, J. Phys. Condens. Matter 21 (2009) 224022.
[6] K. Zhang, M. Uhrmacher, H. Hofsaess, J. Krauser, Magnetic texturing of ferromagnetic thin films by sputtering induced ripple formation, J. Appl. Phys. 103/8 (2008) 83507.
[7] S. Hwang, H.-j. Jin, T.-h. Yoon, J.C. Kim, Homogeneous alignment of liquid crystals on an ion-beam-exposed indium-tin-oxide surface without coating alignment layer, Jpn. J. Appl. Phys. 49 (2010) 121702.
[8] O. Yaroshchuk, R. Kravchuk, A. Dobrovolskyy, L. Qiu, O.D. Lavrentovich, Planar and tilted uniform alignment of liquid crystals by plasma-treated substrates, Liq. Cryst. 31 (2004) 859–869.
[9] T.W.H. Oates, A. Keller, S. Facsko, A. Mücklich, Aligned silver nanoparticles on rippled silicon templates exhibiting anisotropic plasmon absorption, Plasmonics 2 (2007) 47–50.
[10] R. Kravchuk, O. Yaroshchuk, S. Gubarev, A. Dobrovolskyy, A. Evsyukov, I. Protsenko, Nanotopology of polyimide films obliquely treated by plasma beam and liquid crystal alignment, Mol. Cryst. Liq. Cryst. Sci. Technol. 512 (2009) 40–47.
[11] R. Kravchuk, K. Artyushkova, O. Yaroshchuk, Plasma beam alignment of liquid crystals on the bare glass: modification of surface chemical composition, Mol. Cryst. Liq. Cryst. Sci. Technol. 546 (2011) 79–86.
[12] O.V. Yaroshchuk, A.D. Kiselev, R.M. Kravchuk, Liquid-crystal anchoring transitions on aligning substrates processed by a plasma beam, Phys. Rev. E 77 (2008) 031706.
[13] Y. Garbovskiy, L. Reisman, Z. Celinski, R.E. Camley, A. Glushchenko, Metallic surfaces as alignment layers for nondisplay applications of liquid crystals, Appl. Phys. Lett. 98/7 (2011) 073301.
[14] O. Yaroshchuk, R. Kravchuk, L. Dolgov, A. Dobrovolskyy, N. Klyui, E. Telesh, A. Khokhlov, J. Brill, N. Fruehauf, Aging of liquid crystal alignment on plasma beam treated substrates: choice of alignment materials and liquid crystals, Mol. Cryst. Liq. Cryst. Sci. Technol. 479 (2007) 111–120.
[15] O.V. Yaroshchuk, R.M. Kravchuk, S.S. Pogulay, V.V. Tsiolko, H.S. Kwok, The rubbing supplemented atmospheric plasma process for tunable liquid crystal alignment, Appl. Surf. Sci. 257 (2011) 2443–2447.
[16] N. Nadaud, N. Lequeux, M. Nanot, J. Jové, T. Roisnel, Structural studies of Tin-doped indium oxide (ITO) and In4Sn3O12, J. Solid State Chem. 135 (1) (1998) 140–148.
[17] T. Ishida, H. Kobayashi, Y. Nakato, Structures and properties of electron-beam-evaporated indium tin oxide films as studied by X-ray photoelectron spectroscopy and work-function measurements, J. Appl. Phys. 73/9 (1993) 4344.
[18] Y. Ishikawa, H. Nagayama, H. Hoshino, M. Ohgai, N. Shibata, T. Yamamoto, Y. Ikuhara, Transmission electron microscopy study of Sn-doped sintered indium oxide, Mater. Trans. 50 (5) (2009) 959–963.
[19] D. Kalhor, S. Ketabi, Annealing effects on opto-electronic properties of thermally evaporated ITO/Ag/ITO multilayered films for Use in color filter electrodes, World Appl. Sci. J. 6 (1) (2009) 83–87.
[20] D. Kim, Y. Han, J.-S. Cho, S.-K. Koh, Low temperature deposition of ITO thin films by ion beam sputtering, Thin Solid Films 377–378 (2000) 81–86.
[21] M. Libra, L. Bárdoš, Effect of post-deposition vacuum annealing on properties of ITO layers, Vacuum 500 (1988) 455–457.
[22] D.C. Paine, T. Whitson, D. Janiac, R. Beresford, C.O. Yang, B. Lewis, A study of low temperature crystallization of amorphous thin film indium-tin-oxide, J. Appl. Phys. 85/12 (1999) 8445.
[23] Y. Shigesato, D. Paine, A microstructural study of low resistivity tin-doped indium oxide prepared by dc magnetron sputtering, Thin Solid Films 238 (1994) 44–50.
[24] R.M. Bradley, J.M.E. Harper, Theory of ripple topography induced by ion bombardment, J. Vac. Sci. Technol. A 6 (1988) 2390.
[25] S.A. Norris, J. Samela, L. Bukonte, M. Backman, F. Djurabekova, K. Nordlund, C.S. Madi, M.P. Brenner, M.J. Aziz, Molecular dynamics of single-particle impacts predicts phase diagrams for large scale pattern formation, Nat. Commun. 2 (2011) 276.
[26] C.S. Madi, E. Anzenberg, K.F. Ludwig, M.J. Aziz, Mass redistribution causes the structural richness of ion-irradiated surfaces, Phys. Rev. Lett. 106 (2011) 066101.

[27] J.M. Colino, M.A. Arranz, Control of surface ripple amplitude in ion beam sputtered polycrystalline cobalt films, Appl. Surf. Sci. 257 (2011) 4432–4438.
[28] P. Karmakar, S.A. Mollick, D. Ghose, a. Chakrabarti, Role of initial surface roughness on ion induced surface morphology, Appl. Phys. Lett. 93/10 (2008) 103102.
[29] J.-H. Kim, J.-S. Kim, J. Muñoz Garca, R. Cuerno, Role of nonlinearities and initial prepatterned surfaces in nanobead formation by ion-beam bombardment of Au(001): experiments and theory, Phys. Rev. B 87 (2013) 085438.
[30] A. Toma, B. Setina Batic, D. Chiappe, C. Boragno, U. Valbusa, M. Godec, M. Jenko, F.B. de Mongeot, B.S. Batic, F. Buatier de Mongeot, Patterning polycrystalline thin films by defocused ion beam: the influence of initial morphology on the evolution of self-organized nanostructures, J. Appl. Phys. 104/10 (2008) 104313.
[31] A. Keller, S. Facsko, Tuning the quality of nanoscale ripple patterns by sequential ion-beam sputtering, Phys. Rev. B 82 (2010) 155444.
[32] A. Toma, D. Chiappe, B. Setina Batic, M. Godec, M. Jenko, F. de Mongeot, Erosive versus shadowing instabilities in the self-organized ion patterning of polycrystalline metal films, Phys. Rev. B 78 (2008) 153406.
[33] P. Gailly, C. Petermann Tihon, K. Fleury-Frenette, Ripple topography and roughness evolution on surface of polycrystalline gold and silver thin films under low energy Ar-ion beam sputtering, Appl. Surf. Sci. 258 (2012) 7717–7725.
[34] D. Ghose, Ion beam sputtering induced nanostructuring of polycrystalline metal films, J. Phys. Condens. Matter 21 (2009) 224001.
[35] T. Škeren, K. Temst, W. Vandervorst, A. Vantomme, Ion-induced roughening and ripple formation on polycrystalline metallic films, New J. Phys. 15 (2013) 093047.